A spring-supported arch model for predicting the hydrostatic collapse strength of flexible risers with layer gap

Li, Xiao; Jiang, Xiaoli; Hopman, Hans

Publication date
2018

Document Version
Final published version

Published in
Proceedings of the 32nd Asian-Pacific Technical Exchange and Advisory Meeting on Marine Structures (TEAM 2018)

A Spring-Supported Arch Model for Predicting The Hydrostatic Collapse Strength of Flexible Risers with Layer Gap

Xiao Li*[1],Xiaoli Jiang[2], Hans Hopman[3]

1) PhD student 2) Assistant Professor 3) Professor
Department of Maritime and Transport Technology, Delft University of Technology
e-mail: X.Li-9@tudelft.nl

Abstract: Flexible riser is a keyenabler for the oil and gas production in ultra-deep water which transports production fluids between floaters and subsea wells. As oil and production heads to water depths greater than 3000 m, huge hydrostatic pressure may compress the flexible risers into collapse. For the deepwater design of flexible risers, they are required to have sufficient collapse resistance for any abnormal condition of a flooded annulus, e.g. geometric imperfections or residual stress. As one of the geometric imperfections, the gap between the carcass and pressure amour may cause a significant reduction in the collapse strength of flexible risers. However, there is no available analytical model that could take this factor into account. This paper presents a spring-supported arch model to estimate thecollapse strength for the subsea flexible risers with layer gap. The outside pressure amour is regarded as springs which support the detached portion of the inner carcass. Numerical simulation was employed to verify the reliability of this spring-supported arch model for a set of gap width. The predictions of the proposed models agree very well with the numerical results, indicating that the arch model is effective for this layer gap issue.
Keyword:flexible riser, critical pressure, layer gap, wet collapse, ultra-deep water

1. INTRODUCTION

Flexible riser is a pipe-like structure which provides conduits for conveying of hydrocarbons or injection fluid between the wellheads and the floaters[1]. A typical flexible riser is made up of multiple layers with different structural and operational functions, as shown in Fig.1[2]. The metallic layers are designed to take loads while the polymeric layers are added as sealing material[3]. Since the oil & gas production are moving towards ultra-deep water fields, the flexible risers are required to be capable of resisting the high hydrostatic pressure[4]. When excessive external pressure is applied onto the flexible riser, the riser will be collapsed. The minimum collapse pressure is called critical pressure[5].

For the most part, the critical pressure is determined by considering the most extreme loading condition of the flexible riser, which is called “wet collapse”[6]. In this scenario, the seawater floods the annulus through the breached outer sheath and the whole external pressure acts directly on the inner liner. The interlocked carcass layer, which is encased by the pressure armour, is the main component for collapse resistance in this case. Generally, two collapse modes for the innermost carcass would occur once the collapse failure happens, which are referred to“eight mode” and “heart mode” that showed in Fig.2[7]. This paper deals specifically with the eight mode of flexible risers in wet collapse.

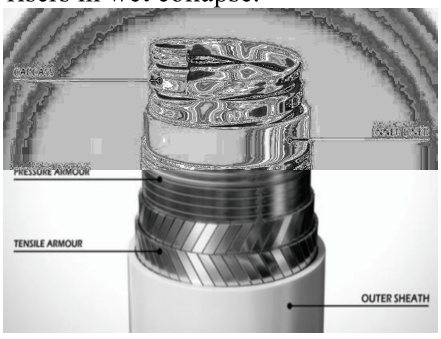

Fig.1 *Main component layers of a flexible riser*[2]

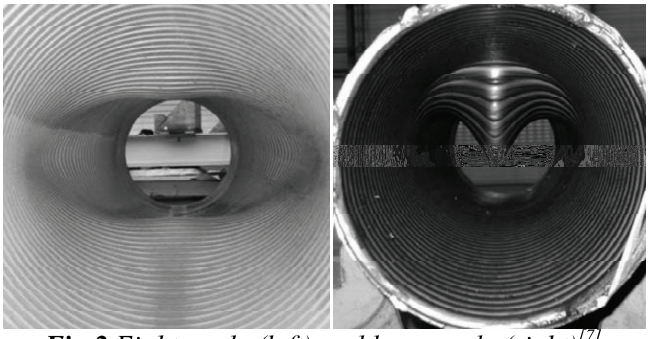

Fig.2 *Eight mode (left) and hear mode (right)*[7]

Normally, the actual critical pressure is higher than the collapse limit of the carcass since the surrounded pressure armour provides it a significant support effect[8]. However, this effect may be reduced by the gap between these two metallic layers. This layer gap is generated from two causes, the volume change of the inner liner and its extrusion into the adjacent interlocked layer[9]. Some researchers pointed out the layer gap may have a significant reduction effect on the critical pressure of flexible risers[9-10].

Fig.3 *Extrusion of the inner liner into the adjacent interlocked carcass[11]*

Up till now, moststudies related to layer gap were limited in numerical investigations which is impractical for design purposes of flexible risers. In this paper, a spring-supported arch model is proposed for the gap-influenced collapse issue. This analytical model could take the gap width into account and give a prediction of the critical pressure for the flexible risers with eight mode collapse. The content of this paper is organized as follows: Section 2 gives a brief introduction of previous collapse studies. Following that, the methodology of the spring-supported arch is presented in Section 3. In Section 4, the reliability of the proposed model is verified by some case studies and the final section concludes the work.

2. PREVIOUS STUDIES

The radial buckling of flexible risers has been studied for years. Mostly, the analytical model for predicting the critical pressure of flexible risers are developed from the ring buckling theories[12]

$$P_{cr} = \frac{3EI}{R^3}, \tag{1}$$

where *EI* is the bending stiffness of the ring and *R* is the ring radius.

Since the flexible pipe is a concentric structure, Glock[13]presented a closed-form analytical solution for the critical pressure of an elastic cylinder that confined in a rigid cavity

$$P_G = \frac{EI}{1-\upsilon^2}\left(\frac{t}{D}\right)^{2.2}, \tag{2}$$

where υ is Poisson's Ratio, *t* is the wall thickness of the cylinder and *D* is the mean diameter.

Glock's formula was then extended by others[14-15]to consider a tightly or loosely fitted concentric rings. Although those formulae could consider the gap effect, they give an overestimated prediction of critical pressure for flexible pipes. This is because the pressure armour supports the carcass more like an elastic medium rather than a rigid cavity. With this regards, an elastic ring model with horizontal spring supports was proposed as[8,16]

$$P_{cr1} = \frac{3E_iI_i}{R_i^3} + \frac{2}{3}\frac{8E_oI_o}{(\pi^2-7)R_o^3} \tag{3}$$

where the subscript $()_i$and $()_o$ represent the inner and outer ring, separately.

The pressure armour is considered as springs in the above model which supports the carcass in the horizontal direction, as shown in Fig.4[8]. However, this model is developed for the flexible risers with no gap in-between and only provides an elastic solution due to the usage of the principle of stationary potential energy. Since the flexible risers are more likely to be collapsed in the plastic range in a deep water condition[16], efforts were made to predict the plastic collapse pressure of the flexible risers with layer gap in this paper.

3. ANALYTICAL MODEL

For the carcass which encased in the pressure armour, the value of the radial gap between these two layers is a key element that affects its anti-collapse strength. Intuitively, a larger gap width leads to a higher reduction of collapse resistance due to a weaker constraint provided by pressure armour. For a flexible riser which possesses a layer gap between the carcass and pressure armour, its progressive buckling process can be described as Fig.5[17].

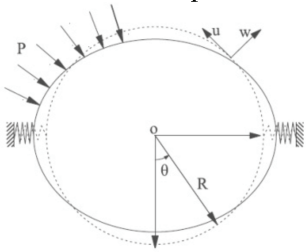

Fig.4 *Buckling of the inner cylinder with spring supports[8]*

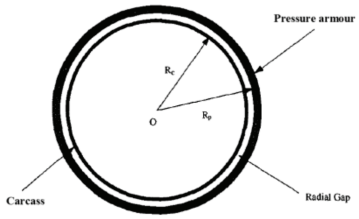

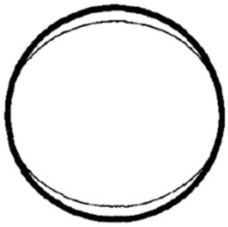

Fig.5 *Progressive buckling process for a symmetrical collapse model[17]*

It can be seen that two phases would occur in this buckling process: pre-contact and post-contact phases. During the pre-contact phase, the carcass is deformed as abuckled single layer ring. Once the contact occurs, the surrounded pressure armour would impose constraints on the inner carcass and thus, the inner carcass layer can be divided into two portions: attached portion and detached portion. In this post-contact phase, the collapse pressure of the inner layer is decided by the buckling strength of the detached portion[18].

These two phases are considered in the analytical model presented in this section. For the pre-contact phase, formulas related to the radial buckling of a single ring are adopted to determine the pressure P_{con} at the contact moment. For the post-buckling phase, the detached portion is regarded as a spring-supported arch which has a buckling pressure P_{arch}. The critical pressure of a flexible riser with layer gap is calculated as the sum of P_{con} and P_{arch}.

Pre-contact phase

For the buckling of a single ring, Timoshenko and Gere assumed that the plastic collapse pressure P_y is the value of the external pressure at which yielding in the extreme fibres of the ring begins[12]. Therefore, it can be calculated as

$$P_y^2 - [\frac{\sigma_y t_c}{R_c} + (1+6\frac{\omega_0}{t_c})P_{cr}]P_y + \frac{\sigma_y t_c}{R_c}P_{cr} = 0, \tag{4}$$

and the maximum horizontal displacement of the point A (see in Fig.6) at the plastic collapse pressure is given as

$$\omega_{\max} = \frac{\omega_0 P_y}{P_{cr} - P_y}, \tag{5}$$

where ω_0 is the initial radial deflection of the ring, σ_y is the material yielding stress, R_c and t_c are mean radius and equivalent thickness of the carcass, P_{cr} is the elastic critical pressure obtained from Eq. (1), t_c is the equivalent thickness of the carcass that can be calculated by referring to [19].

The inner ring would be collapsed as a sing ring if the gap width g_w is large than ω_{max}; otherwise, layer contact happens, followed by the post-contact phase. The pressure at the contact moment can be determined by equating the horizontal displacement ω_1 to the gap width g_w.

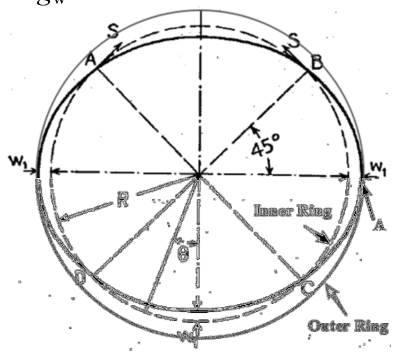

Fig.6 *Contact moment of a concentric ring structure*

Therefore, this pressure is given as

$$P_{con} = \frac{g_w P_{cr}}{(g_w + \omega_0)}, \tag{6}$$

and the bending moment and hoop force at the crown point of the inner ring can be calculated by

$$M_{con} = P_{con} R_c \frac{\omega_0}{1 - P_{con}/P_{cr}}, \tag{7}$$

$$N_{con} = P_{con} R_c, \tag{8}$$

and thus, the maximum compressive stress at the crown point for the contact moment is

$$\sigma_{\max} = \frac{P_{con} R_c}{t_c} + \frac{6 P_{con} R_c}{t_c^2} \frac{\omega_0}{1 - P_y / P_{cr}}, \tag{9}$$

This maximum compressive stress is prepared for the arch model presented in the following post-contact phase.

Post-contact phase

After the carcass contacts with the surrounded pressure armour, the contact point will keep moving upwards until the critical pressure arrives, as shown in Fig.7[17].

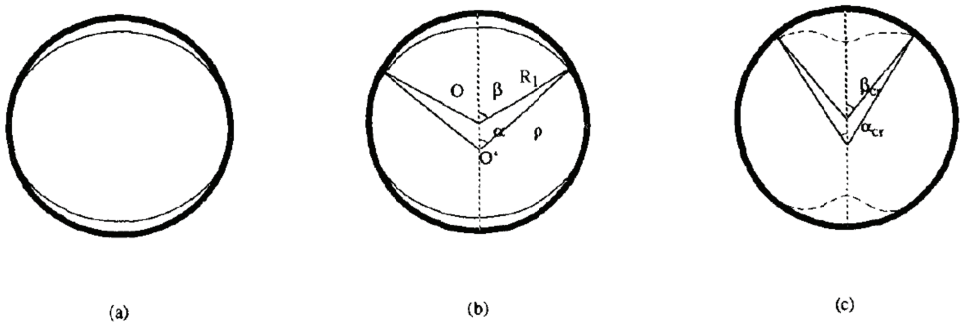

Fig.7 *Progressive buckling process during the post-contact phase*[17]

The detached portion can be regarded as a circular arch with a new centre O'[17]. When the position of the contact point at the collapse moment is determined, the geometry of this circular arch can be calculated by

$$\begin{cases} 2\pi R_c - 2R_{con}(\pi - 2\beta_{cr}) = 4\alpha_{cr}\rho_{cr} \\ \rho_{cr}\sin\alpha_{cr} = R_{con}\sin\beta_{cr} \end{cases} \tag{10}$$

where R_{con} is the distance from the contact point to the ring centre O at the collapse moment, ρ_{cr} is the arch radius referred to the new centre O'; α_{cr} and $\beta_{cr}$are the angular quantities defined in Fig.7 (c).

Since the surrounded pressure armour is treated as springs, then the concentric ring structure could be simplified as a spring-supported arch model, as shown in Fig.8. The general linear equilibrium equation set for the differential element of a circular arch is expressed as[20]

$$\begin{cases} Q'_x - N + q_x\rho_{cr} = 0 \\ N' + Q_x + q_z\rho_{cr} = 0 \\ M' + Q_x\rho_{cr} = 0 \end{cases} \tag{11}$$

where M, N, and Q_x are the bending moment, hoop force and radial shear force on the differential element; q_x and q_z are the uniform loads along the radial and circumferential directions, as shown in Fig.9. In the collapse analysis of flexible risers, values of those loads are given as

$$\begin{cases} q_x = -q = -(P - P_{con}) \\ q_z = 0 \end{cases} \tag{12}$$

where q is the differential pressure between the external pressure P and the pressure at the contact moment P_{con}.

As the linear relationship between strains and displacements is given as

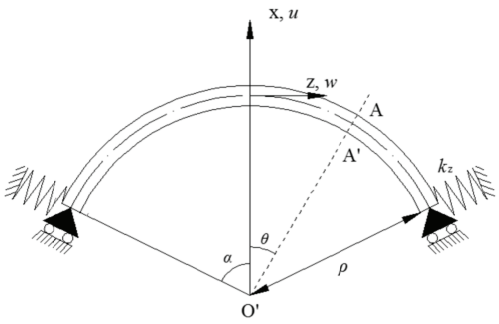

Fig.8 *Spring-supported arch model*

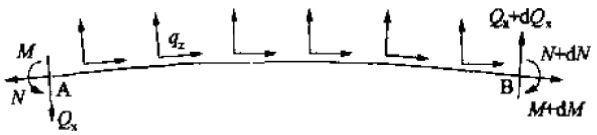

Fig.9 *Equilibrium of a differential element of the arch*[20]

$$\begin{cases} \varepsilon_x = \dfrac{\partial u}{\partial x} \\ \varepsilon_z = \dfrac{\partial w}{\rho_{cr}\partial\theta} + \dfrac{u}{\rho_{cr}} \\ \varepsilon_{xz} = \dfrac{\partial u}{\rho_{cr}\partial\theta} + \dfrac{\partial w}{\partial x} - \dfrac{w}{\rho_{cr}} \end{cases} \tag{13}$$

then the equilibrium equation set Eq.(11) can be redefined with Eq.(12) & (13)

$$\begin{cases} -E_c A_c \dfrac{w'' + u'}{\rho_{cr}} = 0 \\ E_c A_c \dfrac{w' + u}{\rho_{cr}} + \dfrac{E_c I_c}{\rho_{cr}^3}(u^{\mathrm{IV}} + 2u'' + u) = -Rq \end{cases} \tag{14}$$

where u and w are the displacements of the differential element along the radial and circumferential directions, separately; θ is the angle for an arbitrary cross-section of the arch; the items with subscript $()_c$ refers to the parameters of the carcass; ()' represents $\dfrac{\partial}{\partial\theta}$. If taking K as

$$K = -\frac{\rho_{cr}^3}{E_c I_c}(\rho_{cr} q + EA\frac{w' + u}{\rho_{cr}}), \tag{15}$$

Then the general solution of Eq.(14) can be written as

$$\begin{cases} u = KC_1\cos\theta + KC_2\theta\sin\theta + K \\ w = -KC_1\sin\theta - KC_2(\sin\theta - \theta\cos\theta) + KC_3\theta \end{cases} \tag{16}$$

Where C_1~C_3 are constants that determined by the boundary conditions, and therefore, the forces for any arbitrary cross section are given as

$$\begin{cases} N = \dfrac{E_c A_c K}{\rho_{cr}}(1 + C_3) + \dfrac{E_c I_c K}{\rho_{cr}^3}(1 + 2C_2\cos\theta) \\ M = \dfrac{E_c I_c K}{\rho_{cr}^2}(2C_2\cos\theta + 1) \\ Q_x = \dfrac{E_c I_c K}{\rho_{cr}^3}(2C_2\sin\theta) \end{cases}, \tag{17}$$

For a spring-supported arch model as given in Fig.8, it has boundary conditions as follows:
(1) At the crown point θ=0, it should satisfy

$$\begin{cases} u''' + u' = 0 & \text{No shear force} \\ w\big|_{\theta=0} = 0 & \text{No hoop displacement} \\ u' = 0 & \text{No rotation} \end{cases} \tag{18}$$

(2) At the contact point θ=α, it should satisfy

$$\begin{cases} w\big|_{\theta=\alpha} = 0 & \text{No hoop displacement} \\ N_{\theta=\alpha} = R_{con} q & \text{Force equilibrium in hoop direction} \\ Q_x + k_{zp} u = 0 & \text{Force equilibrium in radial direction} \end{cases} \tag{19}$$

where k_{zp} is the elastic stiffness of the pressure amour, which can be obtained by[16]

$$k_{zp} = \frac{9\pi}{4}\frac{E_p I_p}{R_p^3}, \tag{20}$$

where the subscript $()_p$represents the pressure armour.

The boundary condition displayed in Eq.(19b) is based on an basic assumption that given by Jacobsen, which is: the thrust force in the attached portion is constant and equals qR_{con}[21].With the above boundary conditions, the formula of C_1~C_3 can be derived

$$\begin{cases} C_1 = \dfrac{D_5}{D_6} - \dfrac{D_4}{D_3 D_6} k_{zp} \\ C_2 = (\dfrac{1}{D_3} + \dfrac{C_1 \cos\alpha_{cr}}{D_3}) k_{zp} \\ C_3 = \dfrac{C_1 \sin\alpha_{cr} + C_2(\sin\alpha_{cr} - \alpha_{cr}\cos\alpha_{cr})}{\alpha_{cr}} \end{cases} \tag{21}$$

and the coefficients in Eq.(21) can be calculated as

$$\begin{cases} D_1 = \dfrac{E_c A_c}{\rho_{cr}} \\ D_2 = \dfrac{E_c I_c}{\rho_{cr}^3} \\ D_3 = (2D_2 - k_{zp}\alpha_{cr})\sin\alpha_{cr} \\ D_4 = D_1 \dfrac{\sin\alpha_{cr} - \alpha_{cr}\cos\alpha_{cr}}{\alpha_{cr}} + 2D_2\cos\alpha_{cr} \\ D_5 = -(\dfrac{R_{con} q}{K} + D_1 + D_2) \\ D_6 = D_1 \dfrac{\sin\alpha_{cr}}{\alpha_{cr}} + \dfrac{D_4}{D_3} k_{zp}\cos\alpha_{cr} \\ D_7 = \dfrac{\sin\alpha_{cr}}{\alpha_{cr} D_6} + k_{zp} \dfrac{\cos\alpha_{cr}}{D_3 D_6} \dfrac{\sin\alpha_{cr} - \alpha_{cr}\cos\alpha_{cr}}{\alpha_{cr}} \\ D_8 = -\dfrac{k_{zp}}{D_3}[\dfrac{D_4}{D_6}\dfrac{\sin\alpha_{cr}}{\alpha_{cr}} - (1 - \dfrac{D_4 k_{zp}\cos\alpha_{cr}}{D_3 D_6})\dfrac{\sin\alpha_{cr} - \alpha_{cr}\cos\alpha_{cr}}{\alpha_{cr}}] \\ K = \dfrac{(\rho_{cr} - R_{con} D_1 D_7) q}{(D_1 + D_2)(D_1 D_7 - 1) - D_1 D_8} \end{cases} \tag{22}$$

Computing the compressive stress at the crown point of the arch with Eq.(17). Once the compressive stress goes up to the value that given as

$$\sigma_{cr} = \sigma_y - \sigma_{\max}, \tag{23}$$

the material of the carcass reaches its yield stress and the buckling pressure P_{arch} of this arch is determined by

$$\frac{N}{t_c} + \frac{6M}{t_c^2} = \sigma_{cr}, \tag{24}$$

By substituting Eq.(17) into Eq.(24), the buckling pressure $P_{arch}$of this spring-supported arch can be obtained. Finally, the critical pressure of the flexible risers with a layer gap is obtained by

$$P_{cr} = P_{con} + P_{arch}, \tag{25}$$

Contact position at the collapse moment

If the position of the contact point, i.e. R_{con} and β_{cr}, at the collapse moment is determined, the arch geometry can be obtained with Eq.(10), followed by the calculation of the critical pressure with the above-mentioned methods. However, this position is not easy to be determined since it is decided by multiple factors, such as gap width and bending stiffness ratio between the outer and the inner layer. In order to tackle this problem, a formula needed to be proposed to estimate the value of R_{con} at the collapse moment. This formula for R_{con} should meet such rules:

I. R_{con} is approximate to the sum of carcass radius, gap width, and initial deflection when the outer layer becomes infinite rigid;

II. R_{con} is approximate to the sum of carcass radius, gap width, and maximum horizontal displacement ω_{max} when the outer layer's stiffness approaches zero;
III. R_{con} is not affected by the stiffness of the outer layer when $g_w \geq \omega_{max}$.
Therefore, a formula is proposed as

$$R_{con} = R_c + g_w + \omega_0 + (\omega_{max} - g_w)(\frac{g_w + \omega_0}{\omega_{max} + \omega_0})^{\Phi_K}, \quad 0 \leq g_w \leq \omega_{max}, \tag{26}$$

where Φ_K is the bending stiffness ratio that given as[8]

$$\Phi_K = \frac{E_p}{E_c}(\frac{t_p R_c}{t_c R_p})^3, \tag{27}$$

With the value of R_{con} that estimated from Eq.(26), the buckling pressure P_{arch} of the arch can be determined by decreasing the value of β_{cr} (from $\pi/2$ to 0) continually until the bending moments of the attached and detached portion at the contact position equal to each other, as shown in Fig.10. The bending moments for the detached portion can be calculated with Eq.(17). For the attached portion, the bending moment at the contact position is obtained by[12]

$$M_1 = E_c I_c (\frac{1}{\rho_{cr}} - \frac{1}{R_{con}}), \tag{28}$$

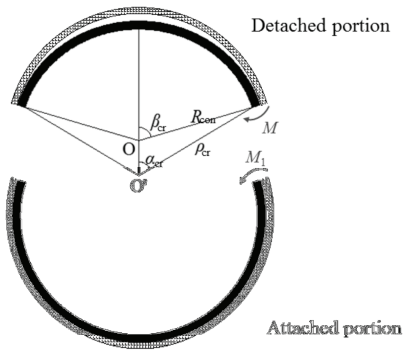

Fig.10 *Bending moments at the contact position*

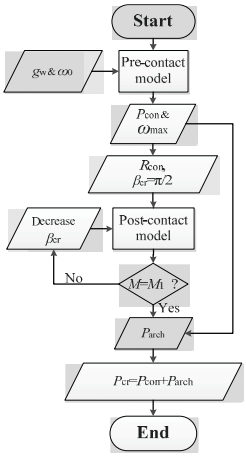

Fig.11 *Flowchart of the whole analysis procedure*

Once M and M_1 are matched, the angle β_{cr} can be determined as well as the buckling pressure P_{arch} of the arch. A flowchart that shows the whole procedure is given as Fig.11.

4. VERIFICATION

In order to verify the reliability of the proposed analytical model, finite element collapse models were built for comparison purpose. Those 2D FE model were developed with Abaqus 6.13 by referring to [22]. The geometric and material data are listed in Table 1. Fig.12 shows an overview of the mesh, the applied load and boundary conditions of the finite element model. More specifically, the pressure loads and boundary conditions are:
1. Pressure load is applied uniformly on the outer surface of the inner ring;
2. Symmetry conditions for the nodes on the x- & y-axis;
3. The ring centre is fully fixed as a pilot node to restrain the free movement and rotation of the concentric ring model.
Three different thicknesses of the outer layer were adopted in the case study –i.e. 4, 5 and 6 mm. For each thickness, the gap width between the inner and outer layers was ranged from 0.01 to 0.5 mm. Therefore, a total 15 cases were carried out for this paper. Those cases were both run by the numerical and analytical models. Table 2 lists the numerical and analytical results of the critical collapse pressure for all the cases.

Table 1*Geometric and material properties of layers[22]*

	Parameter	Carcass	Pressure armor	Unit
geometric	Initial ovalization	0.2%	-	-
	Gap width	Var.	-	mm
	Internal diameter	101.6	Var.	mm
	Layer equivalent thickness	3.97	Var.	mm
material	Young's modulus	192.5	207	GPa
	Poisson ratio	0.3	0.3	-
	Yield strength	600	600	MPa
	Tangent modulus	2000	10483	MPa

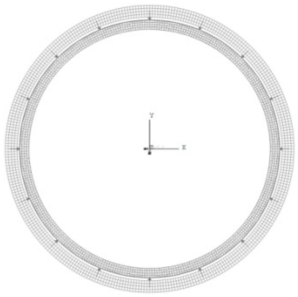

Fig.12 *Load and BCs applied to FEMs*

Table 2 *Numerical and analytical results of the critical pressure for each case*

t_p (mm)		Gap width g_w (mm)				
		0.01	0.05	0.1	0.2	0.5
4	F (MPa)	28.14	27.47	26.74	25.82	23.07
	A (MPa)	28.73	28.01	27.25	25.99	22.81
	Error (%)	2.08	1.95	1.91	0.67	-1.14
5	F (MPa)	33.16	32.34	31.42	29.83	26.28
	A (MPa)	33.75	32.19	30.64	28.26	23.60
	Error (%)	1.78	-0.47	-2.48	-5.23	-10.19
6	F(MPa)	36.12	35.26	34.23	32.42	28.54
	A (MPa)	35.08	33.66	32.23	29.72	24.22
	Error (%)	-2.90	-4.53	-5.84	-8.34	-15.14

From the results listed in Tab.2, it can be seen that the gap width and outer layer thickness have great influences on the anti-collapse strength of the carcass. A 0.5 mm gap width may cause a 20% reduction on the collapse strength of the carcass while this strength could be largely enhanced when the pressure armour becomes thicker.

Additionally, the prediction of the analytical models agrees very well with that of FE models when there is a small layer gap. For the cases with a gap width that is close to zero, the errors are all smaller than 5%. However, the critical pressure predicted by the proposed model gradually deviate from the FEM results with the increase of the gap width and outer layer thickness. For the concentric ring with a gap width of 0.5 mm and an outer layer thickness of 6 mm, the error can be higher than 15%.

The main cause for the above phenomenon is the assumption of thrust force that adopted in boundary condition Eq.(19b). This assumption was proposed by Jacobson[21] for a pipe that encased in a rigid circular cavity. However, the situation is changed for a flexible riser since the pressure armour is not a rigid layer. In this situation, the thrust force at the contact position is governed by multiple factors, e.g. the ovality of the inner layer, the gap width and the stiffness ratio between layers. Therefore, this assumption gives a less accurate estimation of the thrust force at the contact position for the flexible risers with a larger gap width as well as a thinner pressure armour. Finally, large deviations appeared for such cases.

CONCLUSIONS

Layer gap between the carcass and pressure amour has a significant reduction on the anti-collapse strength of flexible risers. Up till now, there are few analytical models that developed for addressing this issue. This paper proposes a spring-supported arch model to predict the wet critical pressure of the flexible riser with layer gap. Numerical simulation was adopted to verify the reliability of the proposed model. The carcass and pressure armour were both considered as rings in these two kinds of models, with the assumption of an eight-shape collapse mode. The prediction from both models showed that the collapse pressure is very sensitive to the stiffness of the pressure amour and the gap width. The anti-collapse strength of a tightly fitted carcass that supported by a stiffer pressure amour could be largely enhanced.

In addition, the proposed model gives an agreeable prediction to the results of numerical simulation for a tightly fitted carcass. For loosely fitted carcass, the accuracy of this model may decrease due to the assumption of the thrust force used in the boundary conditions. The comparison results indicated that the proposed model can be a reliable tool for the flexible risers with stiffer pressure amour and small layer gap.

ACKNOWLEDGEMENTS

This work was supported by the China Scholarship Council [grant number 201606950011].

REFERENCES

[1] Bai, Y., Bai, Q., *Subsea Structure Engineer Handbook*, Houston, USA: Elsevier Inc., (2010).

[2] National Oilwell Varco: *Floating production systems –dynamic flexible risers*, NOV, (2014).

[3] Fergestad, D., et al., *Handbook on Design and Operation of Flexible pipes*, Technical Report, MARINTEK, (2017).

[4] Saglar N., Toleman B., Thethi R., Frontier deepwater developments –the impact on riser systems design in water depths greater than 3000m, in: Proceedings of the Offshore Technology Conference (OTC), Houston, Texas, USA, (2015).

[5] Fernando, U.S., Challenge and solutions in developing ultra-high pressure flexibles for ultra-deep water applications, GE Oil & Gas, (2015).

[6] Gay Neto A., Martins C.A., Flexible pipes: influence of the pressure armour in the wet collapse resistance, *Journal of Offshore Mechanics and Arctic Engineering*, **136**, (2014), 1-8.

[7] Paumier L., Averbuch D., Felix-Henry A., Flexible pipe curved collapse resistance calculation, in: Proceedings of the ASME 28th International Conference on Ocean, Offshore and Arctic Engineering, Honolulu, Hawaii, USA, (2009).

[8] Bai Y., et al., Confined collapse of unbonded multi-layer pipe subjected to external pressure, *Composite Structures*, **156**, (2016), 1-10.

[9] Axelsson G., Skjerve H., Flexible riser carcass collapse analyses –sensitivity on radial gaps and bending, in: Proceedings of the ASME 33rd International Conference on Ocean, Offshore and Arctic Engineering, San Francisco, USA, (2014).

[10] Sousa J.R.M., et al., Equivalent layer approaches to predict the bisymmetric hydrostatic collapse strength of flexible pipes. In: Proceedings of the ASME 37thInternational Conference on Ocean, Offshore and Arctic Engineering, Madrid, Spain, (2018).

[11] Davidson M., et al., Prediction of extruded profile shape of polymer barrier in flexible pipes, in: Proceedings of the 26th International Ocean and Polar Engineering Conference, Rhodes, Greece, (2016).

[12] Timoshenko S.P., Gere J., *Theory of Elastic Stability*. McGraw-Hill, New York, USA, (1963).

[13] Glock D, Uberkritisches verhalten eines starr ummantelten kreisrohres bei wasserdrunck von aussen und temperaturdehnung (Post-critical behavior of a rigidly encased circular pipe subjected to external water pressure and thermal extension), *Der Stahlbau*, **7**, (1977), 212-217.

[14] Boot J.C., Elastic buckling of cylindrical pipe linings with small imperfections subject to external pressure, *Trechless Technology Research*, **12(1-2)**, (1998), 3-15.

[15] Thepot O., Structural design of oval-shaped sewer linings. *Thin-Walled Structures*, **39**, (2001), 499-518.

[16] Chen Y.G., et al., An analytical approach for assessing the collapse strength of an unbonded flexible pipe, *J. Marine Sci. Appl.*, **14**, (2015), 196-201.

[17] Lo K.H., Zhang J.Q., Collapse resistance modelling of encased pipes, *Buried Plastic Pipe Technology*: 2nd Volume, ASTM STP 1222, Dave Eckstein, Ed., American Society for Testing and Materials, Philadephia, (1994).

[18] EI-Sawy K., Sweedan A.M.I., Elastic stability analysis of loosely fitted thin liners –a proposed simplified procedure and evaluation of exisiting solution, *Tunnelling and Underground Space Technology*, **25**, (2010), 689-701.

[19] Martins C.A., et al., Structural behaviour of flexible pipe carcass during launching, in: Proceedings of the International Conference on Offshore Mechanics and Arctic Engineering, Cancun, Mexico, (2003).

[20] Tong G., *In-Plane Stability of Steel Structures*, Beijing, China Architecture & Building Press, (2005).

[21] Jocabsen S., Buckling of circular rings and cylindrical tubes under external pressure, *Water Power*, **26**, (1974), 400-407.

[22] Malta E.R., et al., An investigation about the shape of the collapse mode of flexible pipes, in: Proceedings of the 22nd International Offshore and Polar Engineering Conference, Rhodes, Greece, (2012).